

## Model Systems for the Study of MSWI Fly Ash Thermal Degradation. Kinetics of Active Carbon-Silica Gel Mixtures

Elena Collina<sup>1</sup>, Marina Lasagni<sup>1</sup>, Lorenzo Barilli<sup>2</sup>, Demetrio Pitea<sup>1</sup>

<sup>1</sup>Università Milano-Bicocca, Milano

<sup>2</sup>CAP Gestione s.p.a., Milano

### Introduction

In the last years, thermal behavior of fly ash has been extensively studied<sup>1-3</sup>. Fly ash contains both organic compounds and unburned unextractable carbon (native carbon). We decided to focus our attention on their reactions and did kinetic work on the thermal behavior of municipal solid waste incinerator (MSWI) raw fly ash<sup>4,5</sup> as well as model systems with PCDD, PCDF, PCB parent compounds, *i.e.* Dibenzo-*p*-Dioxin, DD, DibenzoFuran, DF, and BiPhenyl, BPh, and activated carbon, C, mixed with silica, SiO<sub>2</sub><sup>6</sup>. The parent compounds were studied to gain information on the thermal behavior of single compounds and on their reactivity in the absence of dechlorination pathway and metal catalysis; activated carbon as a carbon source was studied in order to understand kinetics and mechanism of fly ash native carbon reactions.

The thermal behavior of MSWI fly ash and model systems was studied in batch experiments in air. A global parameter, Total Organic Carbon (TOC), was used to measure the decrease of reagent concentration in time<sup>7</sup>.

As for the thermal degradation of organic carbon on MSWI fly ash, the only reaction product was CO<sub>2</sub>; it was shown that the carbon for the reactions didn't come from adsorbed organic compounds but from the native carbon matrix of MSWI fly ash. The TOC vs time data were well fitted by the deconvolution treatment and a generalized kinetic model for oxidation of fly ash native carbon was developed. It was shown that the measured conversion of native carbon in fly ashes to CO<sub>2</sub> product is the result of two simultaneous reactions taking place at the fly ash surface: the first reaction is the direct impingement of oxygen onto vacant carbon active sites leading to an immediate carbon gasification; the second one is the dissociative oxygen chemisorption followed by the C(O) complex intermediate gasification. The rate determining step is the intermediate oxidation. The model was validated using

kinetic data for four native fly ashes, three from danish and one from italian municipal solid waste incinerators for temperatures ranging from 200°C to 600°C. The rate constants,  $k_1$ ,  $k_2$ , and  $k_3$  for the three steps together with the activation and thermodynamic parameters were calculated. Fly ashes with a greater initial native carbon concentration behaved differently from those with a lower concentration. The nature of the interaction between native carbon and fly ash were important for the second reaction pathway. The hypothesis that a molecular event of oxygen with a “metallic” site on fly ash surface changed the metal speciation was done.

In the thermal treatment of C-SiO<sub>2</sub> model mixture, the only reaction product was CO<sub>2</sub>. TOC versus time data were well fitted with a single exponential, indicating a first-order reaction. The Arrhenius and Eyring plots showed a piecewise linear trend, thus indicating a change in the reaction rate-determining step. Based on the activation and thermodynamic parameters, the following hypothesis were made: (i) in the lower temperature range (LTR), the direct oxydation reaction is the rate-limiting step; (ii) in the higher temperature range (HTR), the oxygen adsorption and the diffusion processes of surface oxygen complexes are the rate-limiting step. The goal of the studies which followed was to collect new experimental data useful for a better understanding and a validation of the reaction mechanism we proposed for the gasification of native carbon on fly ashes. Particularly, we needed more information on: (i) the effect of initial carbon concentration; (ii) the role of the inorganic matrix. The first objective was achieved through the kinetic study of C-SiO<sub>2</sub> model mixture and, as a reference, of active carbon not supported on a matrix (for the sake of simplicity, we will refer to this system as “free carbon”). In this paper we reported the first results obtained.

## Methods and Materials

**Reagents:** Silica gel, SiO<sub>2</sub>, (Merck, grade 9385, pore diameter 60 Å, surface area 465 m<sup>2</sup>/g, pore volume 1.65 cm<sup>3</sup>/g, 230-400 Mesh) and active carbon, C, (Aldrich, Darco G-60, 100 mesh, powder) were used without any further treatment.

Mixtures of active carbon with silica gel (C-SiO<sub>2</sub>) having initial total organic carbon content, TOC<sup>0</sup>, between 1800 and 7600 ppm were prepared as previously reported<sup>6</sup>.

**Analytical Procedures and Reaction Products:** Details of the analytical method for Total Organic Carbon, TOC, and carbon dioxide, CO<sub>2</sub>, measurements were reported elsewhere<sup>7</sup>. Each reported TOC value was the mean of at least three runs. The reaction products of thermal oxidation of C-SiO<sub>2</sub> mixtures and “free” carbon, C<sub>F</sub>, *i.e.*, active carbon not supported on silica, were determined following the

previously reported procedure<sup>6</sup>. In any case, CO<sub>2</sub> was the only detected reaction product.

**Kinetic Runs:** The thermal treatment of the samples was performed as previously described<sup>4,6</sup>. The kinetics of model mixtures C-SiO<sub>2</sub> was followed as the TOC content decrease in time; that of C<sub>F</sub>, as the weight decrease of the sample. A summary of the experiments was reported in Table 1. To verify the data repeatability, all the runs in set 3 were doubled, with kinetic times in the ranges 0 - 360 min and 0 - 1440 min, respectively; moreover, other runs were repeated randomly. The reproducibility of previously reported results at 1800 ppm<sup>6</sup> was also tested (set 1).

**Table 1:** Thermal degradation of active carbon: summary of the kinetic sets (n = number of runs in a set) performed on C-SiO<sub>2</sub> mixtures and on “free” active carbon, C<sub>F</sub>.

Set (n)	Reagent	TOC <sup>0</sup> (ppm)	T range (°C)	t (min)
1 (2)	C-SiO <sub>2</sub>	1800	350 – 500	0 – 1440
2 (11)	C-SiO <sub>2</sub>	4000	325 – 600	0 – 1440
3 (16)	C-SiO <sub>2</sub>	7600	300 – 600	0 – 1440
4 (5)	C <sub>F</sub>	98 - 250 <sup>a)</sup>	325 – 500	0 – 240

a) Weight (mg) of C<sub>F</sub>.

**Kinetic Data Processing:** The experimental data for the carbon content decrease in time followed a pseudo-first order kinetics both for the model mixtures and the “free” carbon. Kinetic rate constants, k (min<sup>-1</sup>), were calculated with a linear least-squares regression.

The apparent activation and thermodynamic parameters were calculated using Arrhenius and Eyring equations, the goodness of fit was evaluated on the basis of the standard deviation of the least-squares regression parameters ( $\sigma$ ) as well as the determination coefficients (R<sup>2</sup>).

## Results and Discussion

**Effect of temperature on kinetic constants:** The kinetic runs were performed in the range 300 - 600°C on active carbon – silica mixtures, C-SiO<sub>2</sub>, with different initial organic carbon contents, TOC<sup>0</sup>, or on active carbon not supported on silica (“free” carbon, C<sub>F</sub>).

For the runs performed on both C-SiO<sub>2</sub> and C<sub>F</sub>, the TOC - time experimental data followed a pseudo-first order kinetics; in any case, CO<sub>2</sub> was the only detected reaction product.

The rate constants,  $k$  ( $\text{min}^{-1}$ ), were determined and the Arrhenius and Eyring equations were applied. As an example, the Eyring plots were reported in Figure 1. It was possible to observe that the Eyring plots for C-SiO<sub>2</sub> mixtures showed a piecewise linear trend and that the slopes in the Low Temperature Range (LTR) were different, while those in the High Temperature Range (HTR) were almost coincident. On the other hand, the Eyring plot for C<sub>F</sub> was linear over the entire experimental temperature range. The trends observed for the Arrhenius plots were the same.

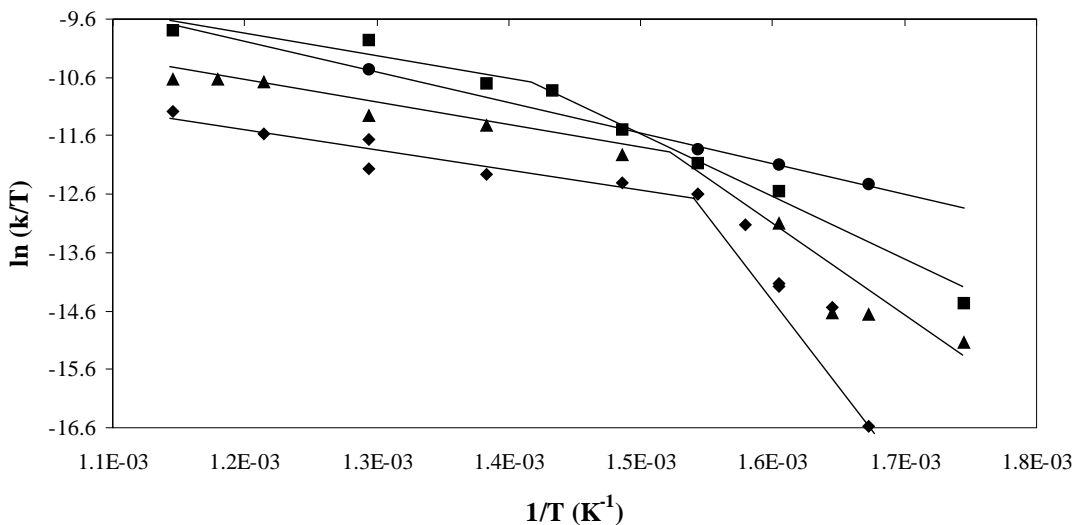


**Figure 1:** Eyring plot for C-SiO<sub>2</sub> mixtures at different TOC<sup>0</sup> values ( $\nu$ , 1800 ppm;  $\sigma$ , 4000 ppm;  $\nu$ , 7600 ppm) as well as for C<sub>F</sub> ( $\lambda$ ).

This observation suggested that, in C-SiO<sub>2</sub> mixtures, the mechanism of the active carbon oxidation below the temperature at which the two straight lines crossed,  $T_{\text{cross}}$ , was different from the one above this temperature. The apparent activation and thermodynamic parameters were calculated and reported in Table 2.

Thus, from the experimental data it was evidenced that the rate constants  $k$  depended on temperature as well as on TOC<sup>0</sup> value. Moreover, from the data processing with Arrhenius and Eyring equations it was shown that both the pre-exponential factor,  $A$ , and the activation energy,  $E_a$ , as well as activation entropy,  $\Delta S^\ddagger$ , and activation enthalpy,  $\Delta H^\ddagger$ , depended on TOC<sup>0</sup> value.

**Table 2:** Activation (using Arrhenius equation) and thermodynamic (using Eyring equation) parameters for C–SiO<sub>2</sub> mixtures and for free active carbon.

Parameter	TOC <sup>0</sup> = 1800 ppm		TOC <sup>0</sup> = 4000 ppm	
	325-370°C <sup>a</sup>	370-600°C	325-410°C <sup>b</sup>	410-600°C
ln (A/min <sup>-1</sup> )	39 ± 8	0.1 ± 0.8	17 ± 3	1.7 ± 0.5
E <sub>a</sub> (kJ mol <sup>-1</sup> )	240 ± 40	34 ± 5	120 ± 20	40 ± 3
R <sup>2</sup>	0.965	0.906	0.948	0.977
ΔS <sup>‡</sup> (kJ K <sup>-1</sup> mol <sup>-1</sup> )	(0.03 ± 0.06)	-(0.294 ± 0.006)	-(0.15 ± 0.03)	-(0.281 ± 0.004)
ΔH <sup>‡</sup> (kJ mol <sup>-1</sup> )	240 ± 40	28 ± 5	120 ± 20	33 ± 3
R <sup>2</sup>	0.903	0.879	0.943	0.968
ΔG <sup>‡</sup> (kJ mol <sup>-1</sup> ) <sup>c</sup>	210 ± 60	240 ± 6	230 ± 30	237 ± 4
% ΔS <sup>‡</sup>	11 ± 3	88 ± 2	48 ± 6	86 ± 2

<sup>a</sup> Temperature T<sub>cross</sub> = 369°C. <sup>b</sup> T<sub>cross</sub> = 411°C. <sup>c</sup> ΔG<sup>‡</sup> at an average temperature of 723 K.

**Table 2 (continued)**

Parameter	TOC <sup>0</sup> = 7600 ppm		C <sub>F</sub>
	325-440°C <sup>d</sup>	440-600°C	325-500°C
ln (A/min <sup>-1</sup> )	13 ± 1	2 ± 1	4 ± 1
E <sub>a</sub> (kJ mol <sup>-1</sup> )	98 ± 7	39 ± 6	49 ± 6
R <sup>2</sup>	0.964	0.883	0.966
ΔS <sup>‡</sup> (kJ K <sup>-1</sup> mol <sup>-1</sup> )	-(0.19 ± 0.02)	-(0.28 ± 0.01)	(0.20 ± 0.01)
ΔH <sup>‡</sup> (kJ mol <sup>-1</sup> )	90 ± 10	32 ± 6	49 ± 6
R <sup>2</sup>	0.918	0.837	0.965
ΔG <sup>‡</sup> (kJ mol <sup>-1</sup> ) <sup>e</sup>	230 ± 10	231 ± 8	190 ± 10
% ΔS <sup>‡</sup>	61 ± 4	86 ± 3	75 ± 4

<sup>d</sup> T<sub>cross</sub> = 439°C. <sup>e</sup> ΔG<sup>‡</sup> at an average temperature of 723 K.

**Empirical equations for the dependence of Arrhenius and Eyring parameters on TOC<sup>0</sup>:** The experimental values of ln A and E<sub>a</sub> showed a linear correlation with (1/TOC<sup>0</sup>) in the LTR as well as in the HTR. Thus, following empirical equations were written:

$$\ln (A)_i = \ln A^0 + \alpha_A (1/\text{TOC}_i^0) \quad (1)$$

$$(E_a)_i = E_a^0 + \varepsilon_E (1/TOC_i^0) \quad (2)$$

where the footer  $i$  indicated experimental values obtained for different  $TOC^0$  values.

Equations (1) and (2) were applied for the processing of the Arrhenius parameters determined for C-SiO<sub>2</sub> mixtures at three different  $TOC^0$  concentrations (Table 2). The regression parameters determined were reported in Table 3. Standard errors ( $\sigma$ ) and determination coefficients ( $R^2$ ) were also reported.

**Table 3:** Dependence of Arrhenius and Eyring parameters on  $TOC^0$ .

Eq.	Parameter	Dimensions	LTR	HTR
(1)	$R^2$		0.983	0.984
	$\ln A^0 \pm \sigma$		$3 \pm 3$	$2.7 \pm 0.2$
	$\alpha_A \pm \sigma$	ppm	$63000 \pm 8000$	$-(4600 \pm 600)$
(2)	$R^2$		0.990	0.826
	$E_a^0 \pm \sigma$	$\text{kJ mol}^{-1}$	$50 \pm 10$	$42 \pm 2$
	$\varepsilon_E \pm \sigma$	$(\text{kJ mol}^{-1}) * \text{ppm}$	$350000 \pm 30000$	$-(13000 \pm 6000)$
(3)	$R^2$		0.990	0.957
	$(\Delta S^\ddagger)^0 \pm \sigma$	$\text{kJ K}^{-1} \text{mol}^{-1}$	$-(0.27 \pm 0.02)$	$-(0.274 \pm 0.003)$
	$\alpha_S \pm \sigma$	$(\text{kJ K}^{-1} \text{mol}^{-1}) * \text{ppm}$	$530 \pm 60$	$-(35 \pm 7)$
(4)	$R^2$		0.993	0.800
	$(\Delta H^\ddagger)^0 \pm \sigma$	$\text{kJ mol}^{-1}$	$40 \pm 10$	$34 \pm 2$
	$\varepsilon_H \pm \sigma$	$(\text{kJ mol}^{-1}) * \text{ppm}$	$350000 \pm 30000$	$-(11000 \pm 5000)$

Empirical equations analogous to eq. (1) and (2) were written for the dependence of Eyring parameters on  $TOC^0$ :

$$[(\Delta S^\ddagger)]_i = (\Delta S^\ddagger)^0 + \alpha_S (1/TOC_i^0) \quad (3)$$

$$[(\Delta H^\ddagger)]_i = (\Delta H^\ddagger)^0 + \varepsilon_H (1/TOC_i^0) \quad (4)$$

The least-squares regression parameters were also reported in Table 3 together with standard errors and determination coefficient.

It was observed that the values determined for the intercepts ( $\ln A^0$ ,  $E_a^0$ ,  $(\Delta S^\ddagger)^0$  and  $(\Delta H^\ddagger)^0$ ) were not significantly different in the LTR and HTR; on the contrary, the

slopes of the regression lines ( $\alpha_A$ ,  $\epsilon_E$ ,  $\alpha_S$  and  $\epsilon_H$ ) have opposite signs in the LTR and HTR and are one-two orders of magnitude higher in the LTR.

**Validation of the empirical equations.** From eq. (1), (2), (3) and (4) and with the parameters reported in Table 3, the values of  $\ln A$ ,  $E_a$  as well as  $\Delta S^\ddagger$  and  $\Delta H^\ddagger$  were calculated for  $\text{TOC}^0 = 1000000$  ppm, *i.e.* a system only constituted by carbon. The calculated data were therefore compared to those determined for  $C_F$  (Table 4).

**Table 4:** Kinetic rate constants,  $k$ , Arrhenius as well as Eyring parameters for  $C_F$  ( $\text{TOC}^0 = 1000000$  ppm): comparison of experimental and calculated values.

	Experimental	Calculated
$k$ ( $\text{min}^{-1}$ , 598 K)	$(2.4 \pm 0.1) 10^{-3}$	$2.3 10^{-3}$
$k$ ( $\text{min}^{-1}$ , 623 K)	$(3.5 \pm 0.4) 10^{-3}$	$3.4 10^{-3}$
$k$ ( $\text{min}^{-1}$ , 648 K)	$(4.7 \pm 0.2) 10^{-3}$	$4.8 10^{-3}$
$k$ ( $\text{min}^{-1}$ , 773 K)	$(2.2 \pm 0.31) 10^{-2}$	$2.1 10^{-2}$
$\ln A$	$3.8 \pm 0.2$	$3 \pm 3$
$E_a$ ( $\text{kJ mol}^{-1}$ )	$49 \pm 1$	$46 \pm 12$
$\Delta S^\ddagger$ ( $\text{kJ mol}^{-1}$ )	$-(0.262 \pm 0.002)$	$-(0.27 \pm 0.02)$
$\Delta H^\ddagger$ ( $\text{kJ K}^{-1} \text{mol}^{-1}$ )	$44 \pm 1$	$39 \pm 11$
$\Delta G^\ddagger$ ( $\text{kJ mol}^{-1}$ ) at 723 K	$233 \pm 2$	$234 \pm 18$
$\% \Delta S^\ddagger$	$81 \pm 2$	$83 \pm 4$

From Table 4 it was observed that the agreement between experimental and calculated values was excellent; moreover there was no detectable difference between the values extrapolated for  $\text{TOC}^0 = \infty$  (*i.e.*, the intercepts, reported in Table 3) and those calculated for  $\text{TOC}^0 = 1000000$  ppm. Thus it was concluded that the proposed model was reliable.

**Theoretical model:** Examples for the dependence of the rate constant on reagent concentrations were already reported<sup>8-10</sup>. The dependence was expressed in terms of surface coverage by means of parameter  $\vartheta_i$ , which represented the fraction of the surface area  $S$  which was covered by the reagent  $i$  at a given concentration value:

$$\vartheta_i = (S_{\text{covered}}/S_{\text{total}}) \quad (5)$$

To take into account this effect, a modified Arrhenius equation was proposed:

$$k = A T^\beta \exp(-E_a/RT) f(\vartheta_1, \dots, \vartheta_N) \quad (6)$$

where usually it was assumed that  $\beta = 0$ ; the function  $f$  determining the dependence of the rate constant on the surface coverage of the  $N$  species present.

Equations such as eq. (6) were useful to relate a change in surface coverage  $\vartheta_i$  only to a change in activation energy  $E_a$  or activation enthalpy  $\Delta H^\ddagger$ . To the best of our knowledge, the experimental results for C-SiO<sub>2</sub> mixtures reported in this paper represented the first case studied where also the parameters  $\ln A$  and  $\Delta S^\ddagger$  depended on the surface coverage.

In our case, the only chemical species present were C atoms ( $N = 1$ ), their initial concentration being expressed in terms of  $\text{TOC}^0$ . Thus, the surface coverage  $\vartheta$  (eq. (5)) was written:

$$\vartheta = (S_{\text{covered}}/S_{\text{total}}) = \text{TOC}^0/\text{TOC}_{\text{max}} \quad (7)$$

where  $S_{\text{covered}}$  was assumed being proportional to  $\text{TOC}^0$  and  $S_{\text{total}}$  was expressed as  $\text{TOC}_{\text{max}}$ , *i.e.* the C concentration necessary for the total coverage of the available surface.

Taking into account eq. (1), (2) and (7), the Arrhenius-like dependence of rate constant  $k$  on temperature and C concentration was written:

$$k = A^0 \exp(\alpha_A/\text{TOC}^0) \exp[-(E_a^0 + \epsilon_E/\text{TOC}^0)/RT] \\ = A^0 \exp(-E_a^0/RT) \exp\{(1/\text{TOC}_{\text{max}}) [\alpha_A - (\epsilon_E/RT)] (1/\vartheta)\} \quad (8)$$

In agreement with experimental results, eq. (8) made evident that the dependence of  $k$  on surface coverage decreased as the fraction of covered surface increased.

Theoretical calculations are now underway to estimate  $\vartheta$  from structure and geometry of active carbon as well as of silica in order to develop a model for the reaction mechanism.

### Acknowledgements

We thank Mr. Massimo Ferri for the valuable work in the laboratory.

### References

- 1 Wikström E., Ryan S., Touati A., Gullett B.K. (2003) *Environ. Sci. Technol.* 37, 1962.
- 2 Hell K., Stieglitz L., Dinjus E. (2001) *Environ. Sci. Technol.* 35, 3892.
- 3 Milligan M.S., Altwicker E.R. (1995) *Environ. Sci. Technol.* 29, 1353.
- 4 Lasagni M., Collina E., Tettamanti M., Pitea D. (2000) *Environ. Sci. Technol.* 34, 130.
- 5 Collina E., Lasagni M., Tettamanti M., Pitea D. (2000) *Environ. Sci. Technol.* 34, 137.
- 6 Lasagni M., Collina E., Tettamanti M., Pitea D. (1996) *Environ. Sci. Technol.* 30, 1896.



- 7 Brocca D., Barilli L., Collina E., Lasagni M., Tettamanti M., Pitea D. (1997) *Chemosphere* 35, 2203.
- 8 Kelemen S.R., Freund H. (1985) *Carbon* 23, 619.
- 9 Kelemen S.R., Freund H. (1985) *Carbon* 23, 723.
- 10 Miessen G., Behrendt F., Deutschmann O., Warnatz J. (2001) *Chemosphere* 42, 609.